Electrocatalysis Hot Paper

International Edition: DOI: 10.1002/anie.201504903
German Edition: DOI: 10.1002/ange.201504903

Stability of Fe-N-C Catalysts in Acidic Medium Studied by Operando Spectroscopy

Chang Hyuck Choi, Claudio Baldizzone, Jan-Philipp Grote, Anna K. Schuppert, Frédéric Jaouen,* and Karl J. J. Mayrhofer**

Abstract: *Fundamental understanding of non-precious metal catalysts for the oxygen reduction reaction (ORR) is the nub for the successful replacement of noble Pt in fuel cells and, therefore, of central importance for a technological breakthrough. Herein, the degradation mechanisms of a model high-performance Fe-N-C catalyst have been studied with online inductively coupled plasma mass spectrometry (ICP-MS) and differential electrochemical mass spectroscopy (DEMS) coupled to a modified scanning flow cell (SFC) system. We demonstrate that Fe leaching from iron particles occurs at low potential (< 0.7 V) without a direct adverse effect on the ORR activity, while carbon oxidation occurs at high potential (> 0.9 V) with a destruction of active sites such as FeN_xC_y species. Operando techniques combined with identical location-scanning transmission electron spectroscopy (IL-STEM) identify that the latter mechanism leads to a major ORR activity decay, depending on the upper potential limit and electrolyte temperature. Stable operando potential windows and operational strategies are suggested for avoiding degradation of Fe-N-C catalysts in acidic medium.*

Polymer electrolyte membrane fuel cells (PEMFCs) are considered as attractive and efficient energy-conversion devices for mobile and stationary applications. At the core of the PEMFC technology, catalysts are essential components especially for overcoming the high activation barrier of the ORR.[1] Today, pure or alloyed Pt is the most efficient class of ORR catalysts. Because of its high costs and scarcity, however, great efforts have recently been made to develop efficient non-precious metal catalysts. State-of-the-art Fe-N-C catalysts prepared by heat treatment of iron, nitrogen, and carbon precursors have now demonstrated substantial ORR activity in acidic environment.[2]

For a successful market introduction, besides activity also stability will be of great importance in order to meet the industry requirements. In the case of Pt/C catalysts, several studies have elucidated the degradation paths,[1a] indicating a complex convolution of mechanisms affecting both Pt nanoparticles and the electron-conductive support, especially at high potential.[3] Compared to the large body of fundamental studies on the degradation of Pt-based catalysts, the instability of Fe-N-C catalysts has hitherto been much less investigated.[4] For porphyrin-derived Fe-N-C catalysts, demetalation of the Fe-based moieties was previously discussed as an origin of the performance degradation.[5] More recently, it has been proposed that carbon corrosion plays a critical role on the integrity of FeN_xC_y moieties, as evidenced by post mortem Mössbauer spectroscopy.[6] Further improvement in the detailed understanding of the degradation mechanisms for Fe-N-C catalysts, in particular by using in situ approaches, is pivotal for the successful design of the next generation of Fe-N-C catalysts for PEMFCs. Therefore, we have investigated in the present work the mechanisms of activity loss of a high-performance Fe-N-C catalyst at various temperatures and potential ranges. Electrochemical techniques have been coupled with advanced online and operando analytical techniques in order to simultaneously investigate Fe leaching and carbon corrosion (see Figure S1 in the Supporting Information).

The Fe-N-C catalyst was synthesized using the sacrificial metal–organic framework approach from a catalyst precursor composed of Fe^{II} acetate, 1,10-phenanthroline, and a Zn^{II} zeolitic imidazolate framework (ZIF-8) in a 1:20:80 mass ratio.[6a] In short, the catalyst precursor was obtained from dry milling of the separate precursors with subsequent heat treatment at 1050 °C in Ar (see Methods in the Supporting Information). As revealed by ^{57}Fe Mössbauer spectroscopy, this catalyst comprises a majority of FeN_x moieties (91 % of the spectral area of Fe) along with minor amounts (9 % of the spectral area of Fe) of metallic Fe (Figure S2 and Table S1). Additional physico-chemical and structural characterizations of the Fe-N-C catalyst are found in Figure S3.

The sensitivity of the catalyst to temperature and certain operational potential ranges is shown in Figure 1 by the change in ORR activity following 2000 and 5000 potential cycles with a rotating disk electrode (RDE) at 900 rpm rotation speed. The initial ORR activity is measured after a short break-in of 20 cycles from 0.0 to 1.0 V. Potentials are noted with respect to a reversible hydrogen electrode (RHE) scale. According to the range of potential cycling (low: 0.1–0.4 V, middle: 0.6–0.9 V, or high: 1.2–1.5 V) and to the electrolyte temperature (20, 50, or 70 °C), the experiments are classified into nine conditions. The initial ORR activities, described in first approximation by their half-wave potential

[*] Dr. C. H. Choi, C. Baldizzone, J.-P. Grote, Dr. K. J. J. Mayrhofer
Department of Interface Chemistry and Surface Engineering
Max-Planck-Institut für Eisenforschung GmbH
Max-Planck-Strasse 1, 40237 Düsseldorf (Germany)
E-mail: c.h.choi@mpie.de
mayrhofer@mpie.de
Dr. A. K. Schuppert, Dr. F. Jaouen
Université de Montpellier
Institut Charles Gerhardt Montpellier
2 place Eugène Bataillon, 34095
Montpellier (France)
E-mail: frederic.jaouen@univ-montp2.fr

Supporting information for this article is available on the WWW under http://dx.doi.org/10.1002/anie.201504903.

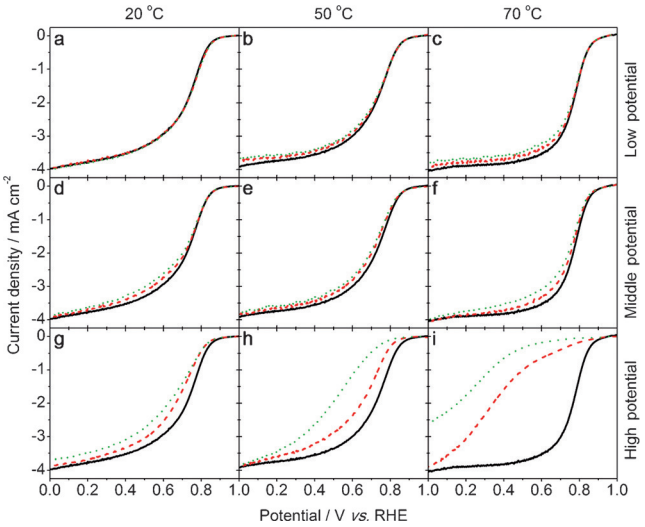

Figure 1. Decay of the ORR activity following potential cycling. The ORR activity in O_2-saturated 0.1 M $HClO_4$ was measured before (solid lines) and after either 2000 potential cycles (dashed lines) or 5000 cycles (dotted lines). The cycling potential range was 0.1–0.4 V (a–c), 0.6–0.9 V (d–f), or 1.2–1.5 V (g–i). The cycling was performed at 20, 50, or 70 °C (first, second, and third column, respectively).

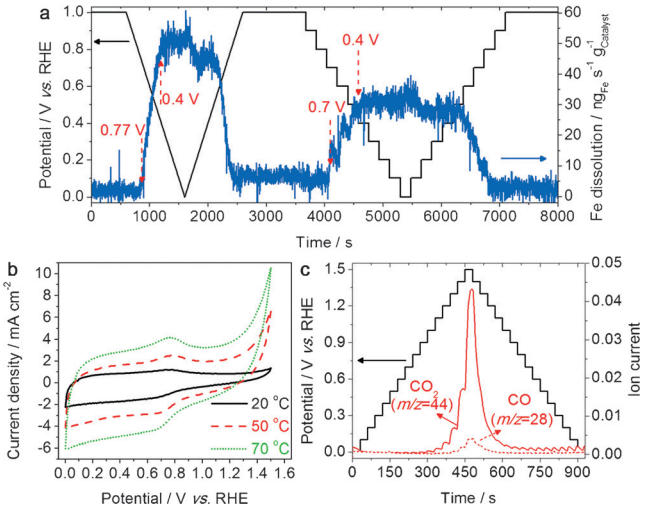

Figure 2. In situ observation of Fe demetalation and carbon oxidation. a) Online SFC/ICP-MS results. The Fe dissolution was recorded at 20 °C during a cyclic voltammogram with 1 mV s^{-1} scan rate and during a stepwise chronoamperometry experiment with a 0.1 V step size. b) Cyclic voltammogram of the Fe-N-C catalyst measured at 50 mV s^{-1} scan rate at various temperatures. c) Online SFC/DEMS results. The DEMS signals were collected during a stepwise chronoamperometry experiment between 0 and 1.5 V at 50 °C. All the experiments were performed in a de-aerated 0.1 M $HClO_4$ electrolyte.

($E_{1/2}$) are 0.74, 0.75, and 0.78 V at 20, 50, and 70 °C, respectively. When cycling in the low-potential range, the $E_{1/2}$ value remains almost unchanged even after 5000 potential cycles, regardless of the electrolyte temperature (Figure 1 a–c). However, ORR activity loss is observed following 5000 cycles at positively shifted potential ranges. The activity decay ($\Delta E_{1/2}$) after 5000 cycles at the middle-potential range amounts to −16, −25, and −26 mV at 20, 50, and 70 °C, respectively. Even more dramatic activity decays are observed after high-potential range cycling, with $\Delta E_{1/2}$ values of −99, −216, and −562 mV after 5000 cycles at 20, 50, and 70 °C, respectively. Hence, these results unambiguously indicate that the ORR activity decay intensifies with a positively shifted potential range and particularly, when combined with an elevated temperature. The small changes of activities at a high current density region after cycling in the low and middle potential range (Figure 1 a–f) may moreover simply be attributed to reduced O_2 permeability in the catalytic film. Reduced O_2 permeability may be an outcome of iron cation contamination of the Nafion ionomer, an effect previously reported for a range of cations on the Pt/Nafion interface.[7]

While this activity decay behavior is not unexpected, the underlying physico-chemical mechanism requires further investigations for clarification. Among the various hypothesized deactivation paths for Fe-N-C catalysts,[5,8] demetalation of the active FeN_xC_y moieties and electrochemical carbon oxidation have been suggested previously. In order to quantify the demetalation of Fe-N-C and resolve whether it is a consequence of carbon oxidation or an independent phenomenon, a central question bearing practical implications for further development, we used a modified SFC connected to online ICP-MS. The real-time ICP-MS signal for the Fe mass being released per mass of catalyst, recorded either under linear or staircase cyclic voltammetry (CV), is shown in Figure 2 a. Surprisingly, while scanning the potential Fe ions start being released from Fe-N-C at about 0.8 V, and the release rate reaches a maximum at 0.4 V. No Fe signal is detected above 0.8 V.

For a non-pyrolyzed Fe–phthalocyanine, it was previously suggested that ferric phthalocyanine could undergo demetalation because of the smaller ionic radius of Fe^{3+} compared to that of Fe^{2+}.[5b] Considering the redox potential of ionic Fe ($E^{o}_{Fe2+/3+} = 0.77\ V_{SHE}$; SHE = standard hydrogen electrode), our results of enhanced iron release at low potential rather suggest that the demetalation process of the Fe-N-C catalysts observed at low potential proceeds from a ferrous species. The Pourbaix diagram of iron indicates that the solid hydroxy oxide $Fe^{III}O(OH)$ species is stable down to a pH of about 1.2 at potentials above 0.77 V_{SHE}.[4] At low pH, the stable species at $E < 0.77\ V_{SHE}$ is the solvated Fe^{2+} cation. These thermodynamic considerations strongly suggest that surface-oxidized metallic iron or iron carbide particles present in the catalyst are responsible for the leaching of Fe observed at low potential (Figure 2 a). The fact that this mechanism of iron leaching results in no ORR activity decay is coherent with the generally accepted view that these iron crystalline structures are inactive or poorly active towards ORR in acid medium, relatively to the ORR activity of FeN_xC_y moieties.[9] Fe-N-C catalysts claimed to comprise solely Fe-based particles and to be free of FeN_xC_y moieties have hitherto shown restricted ORR activity and poor stability in PEMFCs,[10] with the exception of a recent report from Mukerjee's group.[11] In that report, the high ORR activity observed after NH_3 pyrolysis is attributed to N groups that are activated by sub-surface Fe-based crystalline structures. Also, a possible role of Fe-based

particles towards the selectivity of the ORR (2+2 electron mechanism) cannot be completely discarded at this stage. Finally, note that although the results indicate that the release of Fe ions below 0.8 V does not result in a decay of the ORR activity (Figure 1, 1st row), Fe dissolution still remains a crucial issue since it can cause undesired effects on the membrane–electrode assembly (MEA) of a PEMFC system, such as partial exchange of protons in the ionomer of the cathode layer and production of radical oxygen species upon reaction with H_2O_2.[6a,12]

Beside direct demetalation of components of the Fe-N-C catalyst, indirect demetalation might occur by a carbon oxidation mechanism, particularly at a more positive potential range. Namely, CV studies on the Fe-N-C catalyst in a deaerated electrolyte show high oxidation currents at high potentials. The oxidation current increases with temperature (Figure 2b), which correlates well with the increased loss of ORR activity after the cycling at high temperature (Figure 1, 3rd row). To elucidate the origin of the oxidation currents on the Fe-N-C catalyst, online DEMS analysis combined with the SFC system was carried out under chronoamperometric conditions (Figure 2c; CV results of DEMS can be found in Figure S4).[13] The DEMS signal reveals increasing CO_2 ($m/z = 44$) and CO ($m/z = 28$) evolution at high potentials. This demonstrates that both oxidation reactions, $C + 2H_2O \rightarrow CO_2 + 4H^+ + 4e^-$ and $C + H_2O \rightarrow CO + 2H^+ + 2e^-$, occur in the high-potential region, and that carbon oxidation is a major degradation path when Fe-N-C is polarized at high potential. As can be seen in Figure 2c, the onset potentials of carbon oxidation to CO_2 and CO were about 0.9 and 1.2 V, respectively. Considering the thermodynamic potentials (i.e. 0.207 V for CO_2 evolution and 0.518 V for CO), these reactions do not occur until an overpotential of at least +0.7 V is reached. This kinetic stability of carbon at intermediate potentials explains the absence of performance loss after 5000 potential cycles in the low-potential region as well as increased degradation after 5000 potential cycles in the middle- and high-potential regions.

The consequences of carbon oxidation because of high-potential cycling on the structure of Fe-N-C catalyst have been further investigated by means of IL-STEM and IL-energy dispersive X-ray (EDX) spectroscopy analysis.[14] The results reveal considerable changes of the morphology of the catalytic particles in Fe-N-C. Figure 3a and b show dark-field micrographs of an isolated Fe-N-C particle, initially and after 5000 potential cycles in the high-potential range at a temperature of 50 °C. The pristine Fe-N-C particle has a width and height of 537 and 410 nm, respectively. After the potential cycling, thin carbon protrusions located at edges of the Fe-N-C particle disappear, as indicated by the elliptic circles in Figure 3a, and the particle dimensions are reduced to 456 and 391 nm, respectively. This corresponds to a 2D shrinkage of 5–15%, representing an even higher volumetric shrinkage. The weaker contrast of the image after the high-potential cycling might be interpreted either as decreased cluster thickness and/or decreased carbon-wall thickness. However, for the exact measurement of this effect other techniques may be more reliable (i.e. TEM-tomography), as different image settings might affect a true comparison. Nevertheless, the

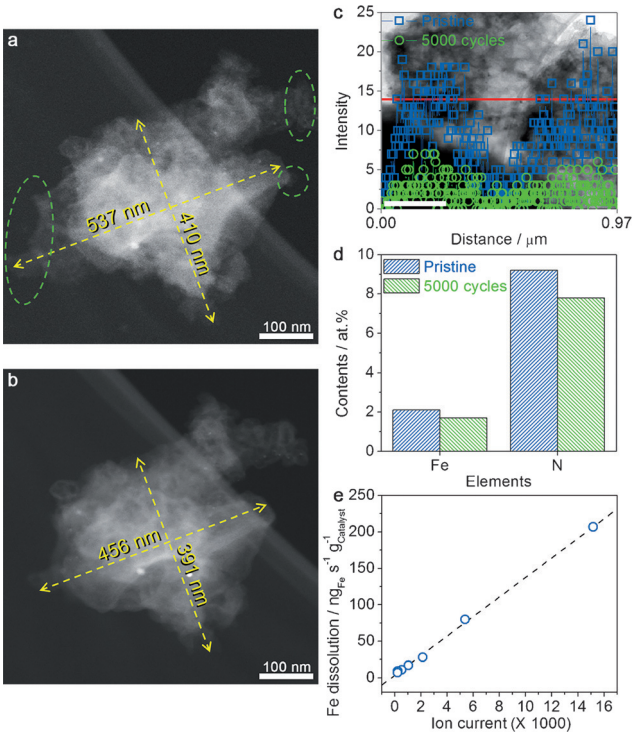

Figure 3. Morphology and composition change of a single Fe-N-C particle. Dark-field IL-STEM micrographs a) before and b) after 5000 cycles performed between 1.2 and 1.5 V at 50 °C in a 0.1 M $HClO_4$ electrolyte. c) Carbon signal in IL-EDX line profiles (scale bar = 250 nm) and d) Fe and N contents before and after high-potential cycling, obtained from IL-EDX data. Acceleration voltage of the electron beam was 200 kV. e) Correlation between the rates of Fe leaching and carbon oxidation at 20 °C (Fe dissolution and DEMS signals were taken from Figure S5).

identical location energy-dispersive X-ray spectroscopy (IL-EDX) line profiles of carbon yield consistently lower signal intensities, supporting the hypothesis of thinned Fe-N-C walls after high-potential cycling (Figure 3c).

The EDX study also shows that the Fe and N contents in the pristine Fe-N-C particle are 2.1 and 9.2 at%, respectively (Figure 3d). The ratio decreases to 1.7 and 7.8 at% after cycling, indicating that carbon corrosion occurring during high-potential cycling also leads to leaching of the elements involved in the structures of the active moieties in Fe-N-C.[6] The loss of Fe in parallel to carbon oxidation is also supported by the detection of Fe signals from the SFC/ICP-MS at potentials above 0.9 V (Figure S5). The intensity of the Fe dissolution signal obtained from the SFC/ICP-MS data is in fact directly proportional to the rate of carbon oxidation obtained from the SFC/DEMS data (Figure 3e). Fe dissolution in the high-potential range is thus for the first time demonstrated to be qualitatively and quantitatively caused by carbon oxidation. Clearly, this Fe dissolution mechanism at high potential is different from the one at low potentials, as it directly impacts the ORR-active moieties and causes a dramatic drop in ORR activity at $T \geq 50$ °C (Figure 1).

Overall, the use of these online techniques has helped us to significantly increase the understanding of the electrochemical degradation paths of Fe-N-C catalysts. In particular,

the direct correlation between carbon oxidation/Fe leaching and ORR activity decay at high electrochemical potential is demonstrated for the first time. However, studies performed in liquid electrolyte and on catalysts operating at very low current density cannot predict all degradation mechanisms occurring in a PEMFC system operating at medium to high current densities. For example, the electrochemical stability of the present Fe-N-C catalyst observed at low to medium potential in liquid electrolyte (Figure 1, 1st and 2nd rows) does not result in a fully stable PEMFC cathode. Indeed, PEMFC stability tests with Fe-N-C cathode catalysts have hitherto exhibited substantial current density losses of about $2\,mA\,cm^{-2}\,h^{-1}$ at 0.4–0.5 V under H_2/O_2[15] or $1–17\,mV\,h^{-1}$ under galvanostatic conditions ($40–400\,\mu V\,h^{-1}$ even on the highly stable Fe-N-C catalysts),[16] while Pt/C shows lower degradation rates of typically $2–10\,\mu V\,h^{-1}$.[17]

Considering this, secondary effects might become dominating in the regular operation range of the PEMFC, that is, below 1.0 V. For instance, while Fe ions dissolving at low electrochemical potential in the liquid electrolyte did not significantly affect the ORR activity per se, they might indirectly lead to the degradation of the catalyst and/or of the Nafion ionomer in a PEMFC system. Dissolved Fe cations can be captured within the Nafion ionomer and/or membrane, resulting in a decreased proton conductivity. More detrimental is the catalytic formation of radical oxygen species by Fe^{2+} in the presence of minute amounts of H_2O_2 produced during the ORR.[12,18]

Taking into account both, direct and indirect degradation effects, we suggest that, ideally, only a limited cathode potential range from approximately 0.7 to 0.9 V should be applied for stable operations of the Fe-N-C catalysts (Scheme 1). Since, in practice, cathode potentials below 0.7 V must be used in order to produce sufficient electric power, the synthesis of Fe-N-C catalysts totally free of reduced metal, metal carbide or metal oxide particles is paramount. This would result in a decreased Fe leaching (or no Fe leaching) at low potential, which is a first requisite for long-term stability in the PEMFC. Alternatively, controlled leaching of such unstable Fe structures before MEA fabrication might be envisaged. For example, a substantial amount of unstable Fe-based structures could be eliminated during the initial activation period (Figure S6). The second degradation path, namely carbon oxidation, could be mitigated under appropriate PEMFC operational conditions, particularly by avoiding excessive high polarization. Moreover, a decrement in temperature, especially during start-up/shutdown procedures,[19] would significantly reduce the carbon oxidation rate during such events.

In conclusion, degradation mechanisms of the Fe-N-C catalyst were studied using an SFC coupled with ICP-MS and DEMS. We have demonstrated that demetalation of Fe species and carbon oxidation occur at low (<0.7 V) and high (>0.9 V) potentials, respectively. Fe demetalation from Fe-based crystalline structures does not directly lead to ORR activity decay, even though it can potentially cause damage to the PEMFC systems. In contrast, oxidation of the carbon-based material to CO_2 and CO, which is significantly accelerated with increasing temperatures and applied potentials, directly leads to the destruction of the carbon surface, and indirectly leads to the destruction of active sites. As a consequence, only a very limited potential window from 0.7 to 0.9 V can be suggested for prolonged operation of this class of catalysts in a first approximation. An extension of this operational window is however possible, and some guidelines for optimization of catalyst design and PEMFC operation based on the insights of these initial results are provided.

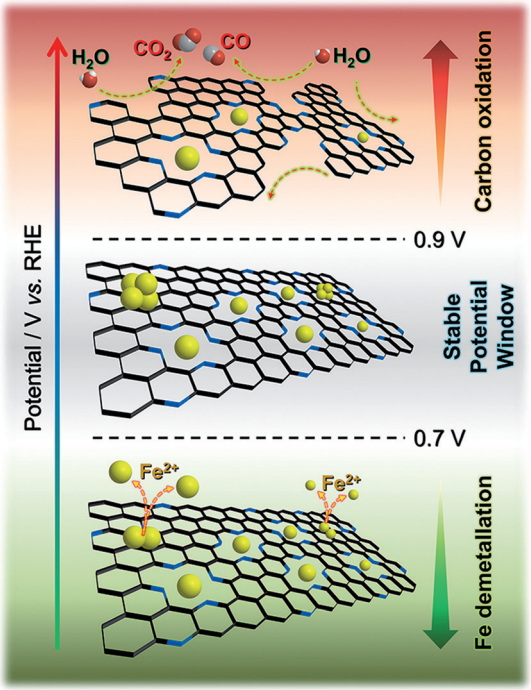

Scheme 1. Scheme describing the deactivation paths of Fe-N-C for different electrochemical potential windows. Blue bars on the honeycomb structures indicate nitrogen atoms doped on the carbon surface. Yellow, red, and white spheres indicate Fe, O, and H atoms, respectively.

Acknowledgements

C.H.C. acknowledges financial support from the Alexander von Humboldt Foundation. C.B. acknowledges financial support from the IMPRS-SurMat doctoral program. A.K.S. acknowledges support from the French Embassy by representation of Campus France. This research was also supported by MAXNET Energy, ANR under contract number 2011CHEX00401, and Basic Science Research Program through the National Research Foundation of Korea (NRF) funded by the Ministry of Education, Science and Technology (grant number NRF-2014R1A6A3A03056182).

Keywords: corrosion · degradation mechanisms · demetalation · electrochemistry · fuel cells

How to cite: *Angew. Chem. Int. Ed.* **2015**, *54*, 12753–12757
Angew. Chem. **2015**, *127*, 12944–12948

[1] a) I. Katsounaros, S. Cherevko, A. R. Zeradjanin, K. J. J. Mayrhofer, *Angew. Chem. Int. Ed.* **2014**, *53*, 102 – 121; *Angew. Chem.* **2014**, *126*, 104 – 124; b) R. Srivastava, P. Mani, N. Hahn, P. Strasser, *Angew. Chem. Int. Ed.* **2007**, *46*, 8988 – 8991; *Angew. Chem.* **2007**, *119*, 9146 – 9149; c) C. Galeano, J. C. Meier, V. Peinecke, H. Bongard, I. Katsounaros, A. A. Topalov, A. H. Lu, K. J. J. Mayrhofer, F. Schüth, *J. Am. Chem. Soc.* **2012**, *134*, 20457 – 20465.

[2] a) Z. Chen, D. Higgins, A. Yu, L. Zhang, J. Zhang, *Energy Environ. Sci.* **2011**, *4*, 3167 – 3192; b) M. Lefèvre, E. Proietti, F. Jaouen, J. P. Dodelet, *Science* **2009**, *324*, 71 – 74; c) G. Wu, K. L. More, C. M. Johnston, P. Zelenay, *Science* **2011**, *332*, 443 – 447; d) E. Proietti, F. Jaouen, M. Lefèvre, N. Larouche, J. Tian, J. Herranz, J. P. Dodelet, *Nat. Commun.* **2011**, *2*, 416; e) Y. Li, W. Zhou, H. Wang, L. Xie, Y. Liang, F. Wei, J. C. Idrobo, S. J. Pennycook, H. Dai, *Nat. Nanotechnol.* **2012**, *7*, 394 – 400; f) N. Ramaswamy, U. Tylus, Q. Jia, S. Mukerjee, *J. Am. Chem. Soc.* **2013**, *135*, 15443 – 15449; g) J. Y. Cheon et al., *Sci. Rep.* **2013**, *3*, 2715; h) J. Tian, A. Morozan, M. T. Sougrati, M. Lefèvre, R. Chenitz, J. P. Dodelet, D. Jones, F. Jaouen, *Angew. Chem. Int. Ed.* **2013**, *52*, 6867 – 6870; *Angew. Chem.* **2013**, *125*, 7005 – 7008; i) C. H. Choi, H. K. Lim, M. W. Chung, J. C. Park, H. Shin, H. Kim, S. I. Woo, *J. Am. Chem. Soc.* **2014**, *136*, 9070 – 9077.

[3] a) R. Borup et al., *Chem. Rev.* **2007**, *107*, 3904 – 3951; b) K. J. J. Mayrhofer, K. Hartl, V. Juhart, M. Arenz, *J. Am. Chem. Soc.* **2009**, *131*, 16348 – 16349; c) K. J. J. Mayrhofer, J. C. Meier, S. J. Ashton, G. K. H. Wiberg, F. Kraus, M. Hanzlik, M. Arenz, *Electrochem. Commun.* **2008**, *10*, 1144 – 1147; d) S. Maass, F. Finsterwalder, G. Frank, R. Hartmann, C. Merten, *J. Power Sources* **2008**, *176*, 444 – 451; e) A. A. Topalov, I. Katsounaros, M. Auinger, S. Cherevko, J. C. Meier, S. O. Klemm, K. J. J. Mayrhofer, *Angew. Chem. Int. Ed.* **2012**, *51*, 12613 – 12615; *Angew. Chem.* **2012**, *124*, 12782 – 12785; f) L. Castanheira, L. Dubau, M. Mermoux, G. Berthome, N. Caque, E. Rossinot, M. Chatenet, F. Maillard, *ACS Catal.* **2014**, *4*, 2258 – 2267; g) L. Castanheira, W. O. Silva, F. H. B. Lima, A. Crisci, L. Dubau, F. Maillard, *ACS Catal.* **2015**, *5*, 2184 – 2194.

[4] D. Banham, S. Ye, K. Pei, J.-i. Ozaki, T. Kishimoto, Y. Imashiro, *J. Power Sources* **2015**, *285*, 334 – 348.

[5] a) M. Lefèvre, J.-P. Dodelet, *Electrochim. Acta* **2003**, *48*, 2749 – 2760; b) H. Meier, U. Tschirwitz, E. Zimmerhackl, W. Albrecht, G. Zeitler, *J. Phys. Chem.* **1977**, *81*, 712 – 718; c) J. A. R. van Veen, H. A. Colijn, *Ber. Bunsen-Ges.* **1981**, *85*, 700 – 704.

[6] a) V. Goellner, C. Baldizzone, A. Schuppert, M. T. Sougrati, K. Mayrhofer, F. Jaouen, *Phys. Chem. Chem. Phys.* **2014**, *16*, 18454 – 18462; b) U. I. Kramm, M. Lefèvre, P. Bogdanoff, D. Schmeißer, J. P. Dodelet, *J. Phys. Chem. Lett.* **2014**, *5*, 3750 – 3756.

[7] a) B. Kienitz, B. Pivovar, T. Zawodzinski, F. H. Garzon, *J. Electrochem. Soc.* **2011**, *158*, B1175 – B1183; b) T. Okada, Y. Ayato, H. Satou, M. Yuasa, I. Sekine, *J. Phys. Chem. B* **2001**, *105*, 6980 – 6986.

[8] a) H. Schulenburg, S. Stankov, V. Schünemann, J. Radnik, I. Dorbandt, S. Fiechter, P. Bogdanoff, H. Tributsch, *J. Phys. Chem. B* **2003**, *107*, 9034 – 9041; b) X. Yu, S. Ye, *J. Power Sources* **2007**, *172*, 145 – 154.

[9] J.-P. Dodelet, R. Chenitz, L. Yang, M. Lefèvre, *ChemCatChem* **2014**, *6*, 1866 – 1867.

[10] a) Y. Hu, J. O. Jensen, W. Zhang, L. N. Cleemann, W. Xing, N. J. Bjerrum, Q. Li, *Angew. Chem. Int. Ed.* **2014**, *53*, 3675 – 3679; *Angew. Chem.* **2014**, *126*, 3749 – 3753; b) J. S. Lee, G. S. Park, S. T. Kim, M. L. Liu, J. Cho, *Angew. Chem. Int. Ed.* **2013**, *52*, 1026 – 1030; *Angew. Chem.* **2013**, *125*, 1060 – 1064; c) Y. Hu, J. O. Jensen, W. Zhang, S. Martin, R. Chenitz, C. Pan, W. Xing, N. J. Bjerrum, Q. F. Li, *J. Mater. Chem. A* **2015**, *3*, 1752 – 1760.

[11] K. Strickland, E. Miner, Q. Jia, U. Tylus, N. Ramaswamy, W. Liang, M.-T. Sougrati, F. Jaouen, S. Mukerjee, *Nat. Commun.* **2015**, *6*, 7343.

[12] A. Pozio, R. F. Silva, M. De Francesco, L. Giorgi, *Electrochim. Acta* **2003**, *48*, 1543 – 1549.

[13] J. P. Grote, A. R. Zeradjanin, S. Cherevko, K. J. J. Mayrhofer, *Rev. Sci. Instrum.* **2014**, *85*, 104101.

[14] N. Hodnik et al., *Phys. Chem. Chem. Phys.* **2014**, *16*, 13610 – 13615.

[15] N. Larouche, R. Chenitz, M. Lefèvre, E. Proietti, J. P. Dodelet, *Electrochim. Acta* **2014**, *115*, 170 – 182.

[16] B. N. Popov, X. Li, G. Liu, J.-W. Lee, *Int. J. Hydrogen Energy* **2011**, *36*, 1794 – 1802.

[17] S. D. Knights, K. M. Colbow, J. St-Pierre, D. P. Wilkinson, *J. Power Sources* **2004**, *127*, 127 – 134.

[18] a) E. Guilminot et al., *J. Electrochem. Soc.* **2007**, *154*, B1106 – B1114; b) V. Goellner, V. Armel, A. Zitolo, E. Fonda, F. Jaouen, *J. Electrochem. Soc.* **2015**, *162*, H403 – H414.

[19] a) Z. Siroma, N. Fujiwara, T. Ioroi, S.-i. Yamazaki, H. Senoh, K. Yasuda, K. Tanimoto, *J. Power Sources* **2007**, *172*, 155 – 162; b) Y. Yu, H. Li, H. Wang, X.-Z. Yuan, G. Wang, M. Pan, *J. Power Sources* **2012**, *205*, 10 – 23.

Received: May 29, 2015
Revised: July 23, 2015
Published online: August 28, 2015

